Stabilization of an optical microscope to 0.1 nm in three dimensions

Ashley R. Carter, Gavin M. King, Theresa A. Ulrich, Wayne Halsey, David Alchenberger, and Thomas T. Perkins

Mechanical drift is a long-standing problem in optical microscopy that occurs in all three dimensions. This drift increasingly limits the resolution of advanced surface-coupled, single-molecule experiments. We overcame this drift and achieved atomic-scale stabilization (0.1 nm) of an optical microscope in 3D. This was accomplished by measuring the position of a fiducial mark coupled to the microscope cover slip using back-focal-plane (BFP) detection and correcting for the drift using a piezoelectric stage. Several significant factors contributed to this experimental realization, including (i) dramatically reducing the low frequency noise in BFP detection, (ii) increasing the sensitivity of BFP detection to vertical motion, and (iii) fabricating a regular array of nanometer-sized fiducial marks that were firmly coupled to the cover slip. With these improvements, we achieved short-term (1 s) stabilities of 0.11, 0.10, and 0.09 nm (rms) and long-term (100 s) stabilities of 0.17, 0.12, and 0.35 nm (rms) in x, y, and z, respectively, as measured by an independent detection laser.

OCIS codes: 170.0180, 180.3170, 170.4520, 170.6900.

1. Introduction

Localization of a single object is not limited by the Rayleigh criterion and has been widely used in single-molecule experiments to resolve nanometer-scale motion of beads,[1] fluorophores,[2] and organelles.[3] The optical imaging of biological systems can also resolve features down to 16 nm,[4] well below the diffraction limit (~220 nm). As both localization and imaging measurements resolve smaller and smaller distances, the physical drift between the microscope objective and the sample becomes increasingly problematic.

Moreover, in surface-coupled optical-trapping experiments,[1,5–7] this unwanted physical drift can be the limiting source of instrumental noise.[8] Yet there is a strong desire to resolve 0.1 nm motion for a myriad of biophysical applications,[9] including measuring[10] and aligning[11] enzymatic motion along DNA with 1 base pair (0.34 nm) resolution. In surface-coupled single-molecule experiments, an enzyme is typically anchored to the surface, while an optically trapped bead, indirectly coupled to the enzyme by a protein and/or a DNA molecule, detects the enzymatic motion [Fig. 1(a)].[12,13] Drift is then coupled into the bead–enzyme distance measurement, obscuring the underlying enzymatic motion. Ideally, such unwanted drift would be eliminated in all three dimensions, since many single-molecule experimental geometries are sensitive to both horizontal and vertical drift.[9,14]

The introduction of a fiducial mark, or a reference point, into the system provides a means to measure and minimize objective-sample drift. Commonly, the fiducial mark is a micrometer-sized bead affixed to the microscope cover slip, the position of which is deduced using video-imaging analysis.[15,16] Such analysis has been used in a feedback loop to stabilize an optical microscope in three dimensions,[15,16] recently achieving ~0.8 nm stabilization in each axis at 25 Hz,[16] though without independent verification.

Compared to video-based techniques, laser-based back-focal-plane (BFP) detection[17,18] offers significantly enhanced bandwidth and potentially better

The authors are with JILA, University of Colorado and National Institute of Standards and Technology, Boulder, Colorado 80309. T. T. Perkins (tperkins@jila.colorado.edu) and G. M. King are also staff members in the Quantum Physics Division, National Institute of Standards and Technology, Boulder, Colorado 80309. T. T. Perkins is also with the Department of Molecular, Cellular and Developmental Biology, University of Colorado, Boulder, Colorado 80309. A. R. Carter is also with the Department of Physics, University of Colorado, Boulder, Colorado 80309. T. A. Ulrich is now with the Department of Bioengineering, University of California, Berkeley, California 94702.

Received 13 July 2006; accepted 18 September 2006; posted 28 September 2006 (Doc. ID 72836); published 20 January 2007.

0003-6935/07/030421-07$15.00/0

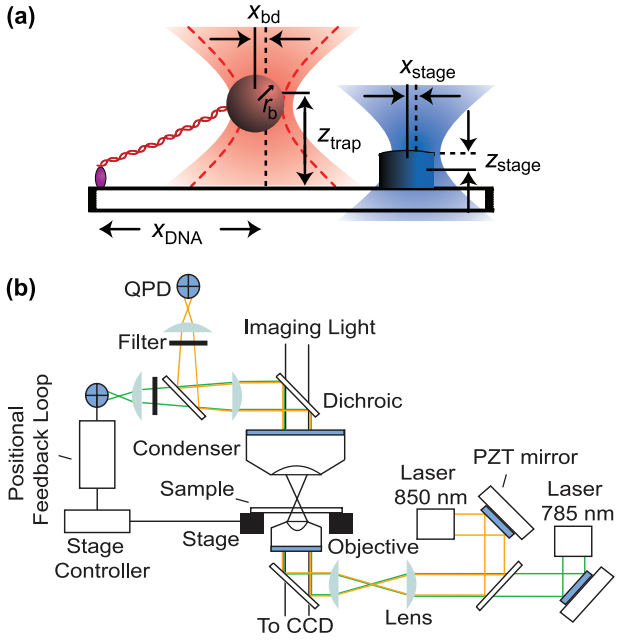

Fig. 1. (a) One application of 3D stabilization is optical-trapping experiments where both horizontal and vertical drift are important. The bead is trapped in a focused laser beam (red dashed curve) and its position is detected by a laser (red). A second laser (blue) measures the fiducial mark position, shown here as a post. (b) Schematic of the 3D stabilization system: QPD, quadrant photodiode; CCD, charge-coupled device; PZT Mirror, closed-loop lead-zirconate-titanate mirror. The blue-shaded components are in optically conjugate planes.

resolution.[19] BFP detection measures the relative position of the laser (set by the objective) to a fiducial mark (attached to the cover slip) in three dimensions[20] and is, therefore, a promising candidate for 3D stabilization of a microscope. While laser-based detection can potentially achieve subpicometer localization of a fiducial mark, instrumental drift, particularly at low frequencies (0.1–100 Hz), limits such measurements.[17,19] Several significant factors contributed to our minimization of this instrumental noise. First, we significantly increased the low-frequency stability of BFP detection. Next, we enhanced the vertical sensitivity of BFP detection. Finally, we fabricated an array of fiducial marks firmly coupled to the cover slip. With these improvements, we stabilized a microscope to 0.1 nm (rms) in each axis over short times (1 s), as measured by an independent detector, while simultaneously achieving a stability of $\leq$0.35 nm (rms) over longer periods (100 s). In comparison with previous real-time stabilization techniques,[16] we achieved an eightfold improvement in each axis at the same temporal resolution, with the added assurance of independent verification.

2. Methods

A. Laser-Based Microscope Stabilization System

The optical microscope used in this study was built upon a microscope body (Nikon TE2000) that was customized to increase its stability as described in earlier work.[8] To actively stabilize this microscope in three-dimensions, we measured the position of a fiducial mark coupled to the stage by using BFP detection[17,18] and applied a feedback loop to keep this position constant [Fig. 1(b)]. More specifically, a laser, focused by the objective (Nikon, PlanAPO-100X-IR, NA = 1.4), scattered off the fiducial mark in the image plane and was collected by the condenser. The scattered laser light interfered with the unperturbed laser beam in the BFP of the condenser, which was imaged onto a quadrant photodiode (QPD, PerkinElmer Optoelectronics, YAG-444-4A; 250 kHz bandwidth with custom electronics; ~40 μW laser power at detector). The fiducial mark's horizontal motion (x, y) relative to the laser was deduced from the normalized intensity difference on the QPD while vertical motion (z) was deduced by the sum signal—the total light falling upon the four quadrants of the QPD.[20] The normalized differences, as well as the offset-amplified sum signal (see Subsection 2.C), were digitized using 16 bits at either 4 or 10 kHz, and the resulting voltages were converted to positions.[8] Measurements were made in an acoustically quiet (NC30), temperature-regulated room (±0.2 °C).

A software-based feedback loop analyzed the position of the fiducial mark and stabilized the microscope by controlling the position of the sample via a lead zirconate titanate (PZT) stage [Fig. 1(b)]. More precisely, the software calculated the average positional signal every 10 ms and generated a proportional error signal. Next, the software digitally outputted the error signal to the stage controller (Physik Instrumente, E-710.P3D) that, in turn, moved the sample via a closed-loop, 3D PZT stage (Physik Instrumente, P517.3CD).

Active stabilization requires a feedback loop. The simple application of feedback loops, without independent verification of their performance, can lead to erroneous conclusions of stability. To understand the necessity of this independent measurement, let us consider one source of instrumental noise that affects BFP detection: laser-pointing instability. Such pointing noise causes apparent motion between the objective and the sample that is compensated for by the feedback loop, leading to added noise that destabilizes the microscope. Without independent verification, there is no knowledge of this noise.[21] Therefore we tracked the position of the fiducial mark with a second laser. To quantify the microscope stability, we calculated the short-term stability by averaging the rms noise within the specified bandwidth (25 to 1 Hz) of 100 consecutive 1 s intervals. The data for presentation were boxcar averaged to 10 Hz except where indicated.

At first, the fiducial marks were 400 nm diameter beads melted onto the microscope coverslip in an epoxy-stabilized flow chamber.[8] Later, we fabricated nanometer-scale glass posts onto cover slips (see Subsection 2.D).

B. Reduction of Low-Frequency Noise in Back-Focal-Plane Detection

More than a decade ago it was shown theoretically that laser-based measurements could achieve subpicometer localization of micrometer-sized beads.[19] However, instrumental drift, particularly at low frequencies, limited such measurements.[17,19] To overcome this instrumental drift, we significantly increased the low-frequency stability of BFP detection by addressing multiple sources of low-frequency laser noise.

Previously, we addressed one source of low-frequency noise, the pointing stability of the detection laser, by using optical fibers to increase the pointing stability.[8] Briefly, we fiber coupled two diode lasers (Blue Sky Research, VPSL, $\lambda = 785$ and 850 nm) that were combined using a dichroic mirror. The 850 nm laser beam could be translated in the imaging plane of the microscope by a two-axis, closed-loop PZT mirror (Physik Instrumente, S330.2SL) imaged onto the BFP of the objective [Fig. 1(b)]. To reduce air currents, optics external to the microscope were enclosed in a box. Additionally, beams were enclosed with 2.5 cm tubes wherever possible.

However, fiber coupling a laser translates pointing instability into intensity noise. Additionally, coupling a laser into a single-mode fiber translates mode fluctuations into intensity noise. This added intensity noise will adversely affect position measurements, particularly in z. To minimize the effects of these noise sources plus polarization noise, we passed a temperature-stabilized,[22] optically isolated diode laser sequentially through an acousto-optic modulator (AOM); a single-mode, polarization-maintaining fiber; and a polarizing beam splitter (PBS) [Fig. 2(a)]. Then 10% of the intensity was sampled onto a large area ($d = 10$ mm) photodiode (PerkinElmer Optoelectronics, YAG-444-A). This photodiode signal was analyzed by using custom-built electronics (200 kHz bandwidth) that output a voltage signal to the AOM driver (Isomet, A232-2). In this manner, a number of noise sources (pointing, mode, and polarization) were minimized by translating them into intensity noise that was also minimized, in turn, by the intensity feedback loop.

To verify the performance of this intensity feedback loop, we sampled 10% of the intensity (I) onto a second photodiode [PD2 in Fig. 2(a)]. Voltages from this second PD were digitized at 20 kHz, boxcar averaged to 100 Hz, and normalized. Without stabilization, I fluctuated 2.5% peak-to-peak for the 785 nm diode laser [Fig. 2(b)], greater than the manufacturer's specification of 0.5% peak-to-peak fluctuation. Yet measurements of I before the AOM were within specification. Thus the excess noise arose from one or more other noise sources (pointing, mode, or polarization). With stabilization, we decreased the intensity noise measured at PD2 by 580-fold to achieve a normalized stability of 1.7×10^{-5} rms at 100 Hz for our 785 nm diode.[23] This result demonstrates the effectiveness of our scheme whereby a variety of noise sources can be systematically minimized without directly measuring and individually addressing each one.

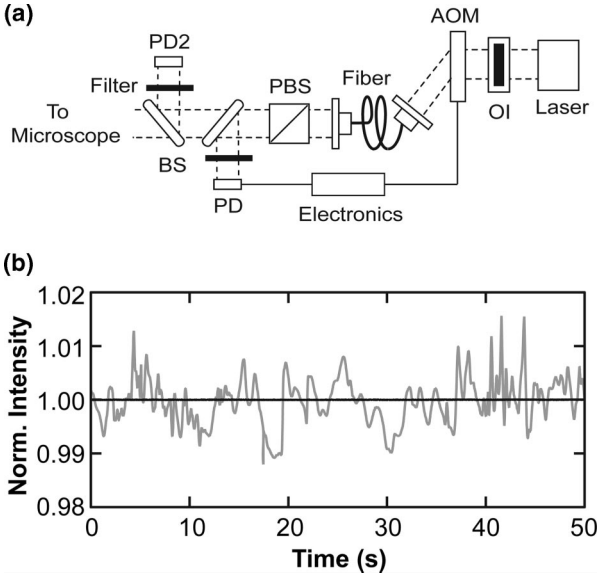

Fig. 2. Low-frequency noise reduction. (a) Optical layout of the intensity feedback loop: OI, optical isolator; PD, photodiode; BS, beam sampler; PBS, polarizing beam splitter; AOM, acousto-optic modulator. (b) Laser intensity prior to stabilization (gray) and after stabilization (black). Data were boxcar averaged to 100 Hz.

C. Enhancement of the Vertical Sensitivity in Back-Focal-Plane Detection

Before demonstrating active stabilization, we needed to enhance the vertical sensitivity of BFP detection. The z positional signal of BFP detection is deduced from the sum voltage of the QPD.[20] This vertical signal arises because of the Guoy phase shift at the focus of the laser. The scattered light off the fiducial mark samples this phase shift. As a result, the sum signal is modulated by constructive or destructive interference between the detection laser and the forward propagating scattered light. This interference leads to a small modulation on top of a comparatively large signal proportional to I. Hence, fluctuations in I appear as fluctuations in z.

The inherent sensitivity (volts per nanometer) of BFP detection is small (0.2 mV/nm), as deduced by moving the fiducial mark vertically through the laser focus [Fig. 3(a), purple]. To increase this sensitivity, we used an offset amplifier to optimally match the variable portion of the sum signal to the 20 V dynamic range of a standard 16-bit data acquisition [Fig. 3(a), black]. More precisely, we subtracted a stable, externally supplied reference voltage (V_0) from the original sum signal (V_z) and multiplied the resulting difference by a 135-fold gain (g) [e.g., $g(V_z - V_0)$]. This amplification led to an enhanced sensitivity of 27 mV/nm, sufficient to resolve 0.1 nm motion. Finally, the combination of offset amplification with intensity stabilization yielded an additional benefit: the small, periodic oscillations in the sum signal were

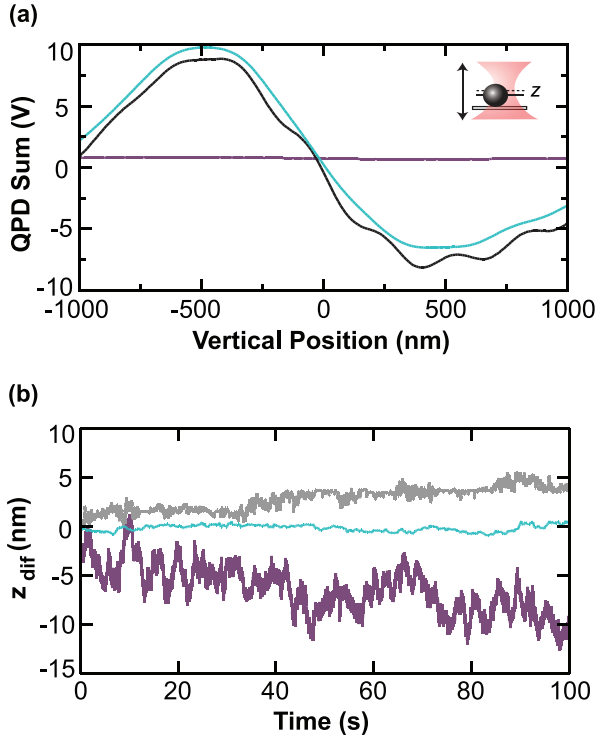

Fig. 3. Vertical BFP detection enhancement. (a) Height calibration signals for an affixed bead that was scanned vertically through the detection laser. The traces represent the inherent signal (purple), offset-amplified signal (black), offset-amplified signal with intensity servo active (blue). (b) Differential BFP detection measurements of vertical motion ($z_{dif} = z_{785} - z_{850}$) using two lasers and one affixed bead as a fiducial mark. Traces represent the inherent signal (purple), the intensity-stabilized signal (gray), and the offset-amplified signal with intensity servo active (blue). Traces displaced vertically for clarity.

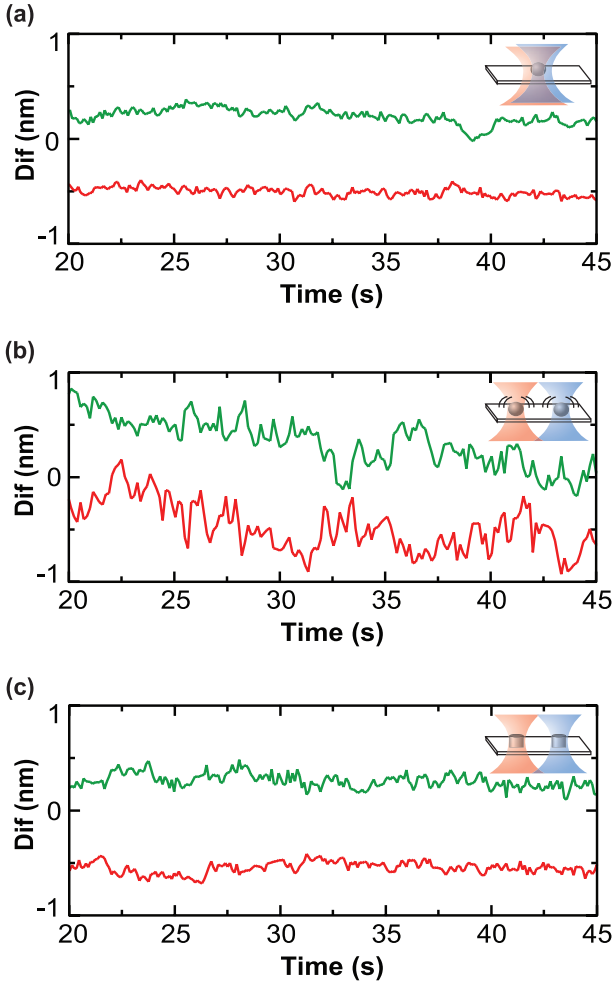

Fig. 4. Fiducial mark movement. (a) Differential BFP detection in x ($x_{dif} = x_{785} - x_{850}$, green) and y ($y_{dif} = y_{785} - y_{850}$, red) using both lasers to measure the position of one affixed bead as a fiducial mark (inset). (b) Differential BFP detection as in (a) except that the lasers measure the position of different affixed beads (inset). The displayed trace reflects the median short-term noise observed in ten trials. (c) Differential BFP detection as in (a) except that the lasers measure the position of two nanofabricated posts (inset). Traces displaced vertically for clarity.

eliminated (blue). Since the PD in the servo loop measures forward propagating light and stabilizes the intensity before it enters the microscope, these oscillations are not the interference between forward-scattered light from the bead, the cover slip, and the primary laser.[24] Such an interaction occurs within the microscope and propagates forward. Therefore we speculate that these oscillations, which are repeatable, result from a small amount of reflected light that feeds back into the diode laser cavity, making it through both the AOM and the optical isolation system.

Before demonstrating active stabilization, we needed to verify that our combination of improvements in optical and mechanical design were sufficient to resolve 0.1 nm motion. We tested our vertical resolution by using differential BFP detection.[8] In this technique, the position of one fiducial mark (initially, a 400 nm diameter bead melted to the cover slip) can be measured with two detection lasers. The difference in the position records is calculated (e.g., $z_{dif} = z_{785} - z_{850}$), which computationally removes stage drift.[8] Thus even after removing such drift, the original z signal was shown to be too noisy to achieve 0.1 nm stability in z_{dif} [Fig. 3(b), purple]. This excess noise was primarily due to the sum signal being proportional to I. The intensity-stabilized z_{dif} signal showed marked improvement but did not achieve our desired 0.1 nm stability [Fig. 3(b), gray]. By coupling intensity stabilization with offset amplification of the BFP vertical signal, we achieved a 0.1 nm differential vertical stability [Fig. 3(b), blue]. More quantitatively, the average short term (1 s) vertical stability was 0.10 nm ($\bar{\sigma}_z$), determined from a nonoverlapping series of one-hundred 1 s intervals (see Subsection 2.A). Long-term vertical stability was ≤0.33 nm (rms) over 100 s. As shown in Fig. 4(a), short-term, horizontal differential stability was excellent, achieving picometer-scale stability ($\bar{\sigma}_x = 40$ pm, $\bar{\sigma}_y = 40$ pm).

D. Reduction of Fiducial Mark Movement

These enhancements of the BFP detection's sensitivity and stability can stabilize a microscope to 0.1 nm only if the fiducial marks are firmly coupled to the

cover slip at this scale. Previously[8] and in Fig. 3, 400 nm diameter polystyrene beads, melted to the cover slip, were used as fiducial marks. Unfortunately, our melted beads still demonstrated significant motion. When differential BFP detection or video-based detection is used to detect the position of one bead, bead movement relative to the surface is undetected [Fig. 4(a)]. However, if differential BFP detection is used to detect two beads, then bead movement relative to the cover slip is visible. In fact, in ~80% of our traces, beads moved >0.1 nm relative to the cover slip [Fig. 4(b)]. Such motion limited our ability to stabilize the microscope and presumably limited the stability of the work of others as well, though in such cases this added motion would have been unseen without an independent measurement.

To surmount these challenges, we fabricated a regular array of fiducial marks that were an integral part of the cover slip. Symmetric nanoscale posts were fabricated on cover slips using hydrogen silsesquioxane (HSQ, Dow Corning, FOx-16) and *e*-beam lithography. First, acid cleaned cover slips were spin coated at speeds of 1–5 krpm with HSQ to produce posts with heights ranging from ~400–1000 nm. Then, thin aluminum films (~15 nm) were vapor deposited to prevent charging during the next step, *e*-beam lithography (38 keV, 450 $\mu C/cm^2$ dose). When exposed to electron irradiation, HSQ crosslinks to form glasslike features as small as 20 nm.[25] This fine control allows for highly symmetric, circular structures to be fabricated. Asymmetric structures lead to cross talk between the x and y motions on the QPD (data not shown). After *e*-beam exposure, the aluminum was etched (~10 s, 16 parts phosphoric acid : 1 part nitric acid : 1 part acetic acid : 2 parts water), and the HSQ was developed (~10 min) by using tetramethyl ammonium hydroxide (TMAH). Finally, to ensure the HSQ was fully crosslinked, it was thermally cured at 600 °C for 15 min.

These posts yielded excellent optical signals with sensitivities in x, y, and z sufficient for 0.1 nm resolution and were, as expected, stable relative to the cover slip [Fig. 4(c)]. To elucidate how these sensitivities scaled with both height (h) and width (w), we constructed a range of posts with varying h (300–1000 nm) and w (300–725 nm). We then measured the sensitivity of each post by translating the post (via the stage) through the laser beam to generate a position versus voltage curve, the slope of which is the sensitivity. In Fig. 5(a), we show these calibration curves for posts of different w. Interestingly, the horizontal and vertical sensitivities scaled with the volume of the post, agreeing with modeling of the post as a point with a polarizability proportional to its volume, even though the dimensions for larger posts were comparable to the laser's wavelength (785 nm).[18,20]

As an alternative to posts, we also investigated holes as fiducial marks. We made holes by spin coating cleaned coverslips with polymethyl methacrylate (PMMA) (~300 nm thick) and then vapor depositing a thin layer of aluminum, as before. Next, a chromium layer was deposited to the cover slip's backside, to prevent etching of the cover slip. Then, we exposed a grid of filled circles with varying radii using *e*-beam lithography (38 keV, 350 $\mu C/cm^2$ dose). After removing the aluminum and developing the resist, we etched the underlying cover slip with buffered hydrofluoric acid to obtain isotropic holes. Finally, the cover slips were cleaned in methyl isobutyl ketone.

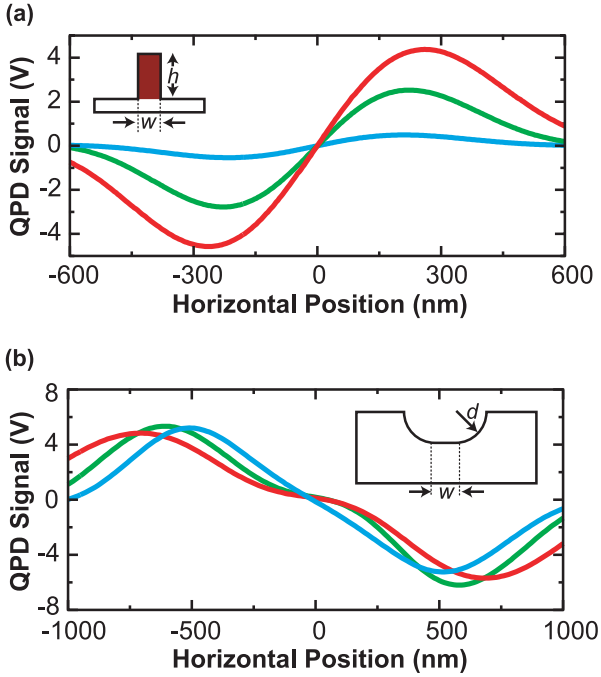

Fig. 5. Fiducial mark signals. (a) Horizontal response for posts of varying size. Posts were a constant height $h = 600$ nm with widths (w) of 350 nm (cyan), 550 nm (green), or 725 nm (red). Inset, geometry of a post. (b) Horizontal response for holes of varying size. Holes were a constant depth $d \cong 500$ nm with initial widths (w) of 100 nm (cyan), 200 nm (green), or 300 nm (red). Inset, geometry of a hole.

Holes, initiated from different openings w in the PMMA, gave different signals [Fig. 5(b)]. For the smallest openings investigated (100 nm), we measured an approximately linear signal over an extended range. However, for larger openings, the response was nonlinear in the middle of the hole. We conclude that hemispherical holes yielded high quality signals, but flat-bottom holes did not. Additionally, holes have their optical center ~1 μm below the plane of the trapped bead, which requires detector beam foci to be in different planes, an added complication. For these reasons, we chose to use posts for future work.

3. Results

A. Active Stabilization

To actively stabilize the microscope, we monitored a post's position with the 785 nm diode laser. The stage position was updated at 100 Hz to keep the post's position constant in all three axes. The 850 nm de-

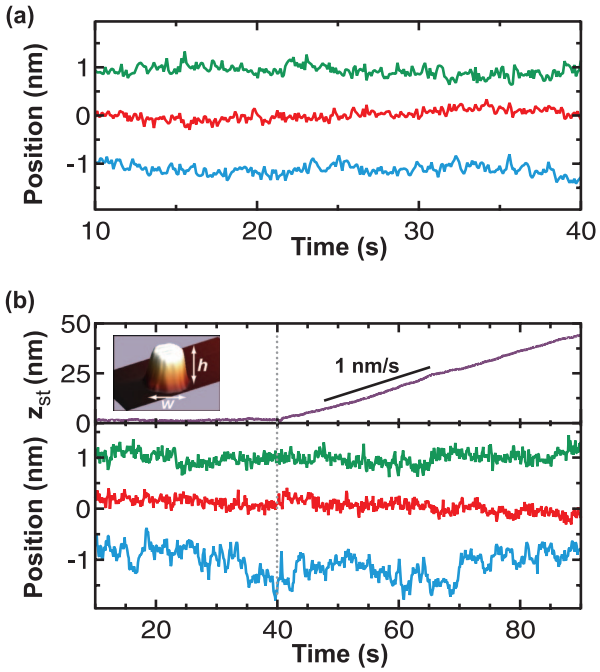

Fig. 6. Active stabilization. (a) Post position measured by the independent 850 nm detection beam, x_{850} (green), y_{850}, (red), and z_{850} (blue). (b) As in (a), independent position records with active stabilization before and during heating. At 40 s, the objective was heated, leading to significant vertical drift that was compensated for by moving the PZT stage (e.g., z_{st}, purple, vertical stage position). Traces displaced vertically for clarity. Inset, atomic force microscope image of a post with a height of 600 nm.

tector, recording the same post, independently determined microscope stability [Fig. 6(a)]. Remarkably, we achieve short-term stabilities, as analyzed above, of $\bar{\sigma}_x = 0.11$ nm, $\bar{\sigma}_y = 0.10$ nm, and $\bar{\sigma}_z = 0.09$ nm, and long-term stabilities of $\sigma_x = 0.17$ nm, $\sigma_y = 0.12$ nm, and $\sigma_z = 0.35$ nm over a 100 s period. We note that the bandwidth of our feedback loop is limited by the resonance frequency of the stage (450 Hz horizontal and 1100 Hz vertical). New, stiffer direct-drive piezoelectric stages with higher resonances should lead to lower noise and higher bandwidth stabilization. Additionally, we note that this independent verification of microscope stability, once performed, is not necessary in stabilization applications.

B. Active Stabilization in the Presence of Significant Heating

The robustness of this 3D stabilization was demonstrated by introducing a large, temporally controllable drift by heating the objective, which has a transmission of 59%,[26] with a high-power, 1064 nm laser (not shown). This type of perturbation is often found in optical-trapping assays,[9,12,13] and a similar motion arises from the common problem of objective settling. Initially, we actively stabilized the microscope at a constant low laser power (50 mW) [Fig. 6(b)]. At 40 s, the laser power was increased by a factor of 3 to 150 mW. During the following 50 s, the active stabilization compensated for the objective's thermal expansion[27] by moving the PZT stage 44 nm to keep the vertical position of the post constant [Fig. 6(b), purple]. Thus in the absence of this correction, there would have been a total vertical drift of 44 nm. Notably, active stabilization yielded excellent long-term stability [0.15, 0.14, and 0.26 nm (rms) over 50 s for σ_x, σ_y, and σ_z]. Short-term stability (1 s) was essentially unchanged at 0.11, 0.10, and 0.10 nm for $\bar{\sigma}_x$, $\bar{\sigma}_y$, and $\bar{\sigma}_z$.

4. Conclusions

The experimental advances presented here allow real-time, 0.1 nm stabilization of an optical microscope in three dimensions. The excellent long-term stability enables high resolution measurements that would previously have been dominated by instrumental drift. Thus we anticipate that the advances developed here will be especially useful in the many surface-coupled single-molecule assays where tracking particles undergoing Brownian motion to nanometer or subnanometer precision is important in determining the fundamental step size of molecular motors.[2,5,6,12,28,29] High-resolution, tethered-particle-motion assays would also benefit from the enhanced stability afforded by this technique.[30] Further, we anticipate that a scanning probe microscope tip could be actively stabilized relative to a fiducial mark engineered into the sample by backscattering light[31] off both these objects. Hence this approach of using nanofabricated fiducial marks in an active, real-time feedback loop to achieve atomic-scale stabilization in three dimensions could be applied to many interesting ultrastable measurement platforms.

The authors thank Jan Hall and Terry Brown for the servoelectronics design, Carl Sauer for custom electronics, and Dan Schmidt for nanofabrication guidance. This work was supported by a Burroughs Wellcome Fund Career Award in the Biomedical Sciences (TTP), an Optical Science and Engineering Program NSF-IGERT grant (ARC), a National Physical Science Consortium Fellowship (ARC), a National Research Council Research Associateship (GMK), a W. M. Keck Grant in the RNA Sciences, and the National Science Foundation (Phy-0404286 and Phy-0096822). Any mention of commercial products is for information only; it does not imply NIST recommendation or endorsement, nor does it imply that the products mentioned are necessarily the best available for the purpose.

References and Notes

1. K. Svoboda, C. F. Schmidt, B. J. Schnapp, and S. M. Block, "Direct observation of kinesin stepping by optical trapping interferometry," Nature **365,** 721–727 (1993).
2. A. Yildiz, J. N. Forkey, S. A. McKinney, T. Ha, Y. E. Goldman, and P. R. Selvin, "Myosin V walks hand-over-hand: single fluorophore imaging with 1.5-nm localization," Science **300,** 2061–2065 (2003).
3. C. Kural, H. Kim, S. Syed, G. Goshima, V. I. Gelfand, and P. R. Selvin, "Kinesin and dynein move a peroxisome *in vivo:* a tug-of-war or coordinated movement?" Science **308,** 1469–1472 (2005).

4. V. Westphal and S. W. Hell, "Nanoscale resolution in the focal plane of an optical microscope," Phys. Rev. Lett. **94,** 143903 (2005).
5. J. T. Finer, R. M. Simmons, and J. A. Spudich, "Single myosin molecule mechanics: piconewton forces and nanometre steps," Nature **368,** 113–119 (1994).
6. A. D. Mehta, R. S. Rock, M. Rief, J. A. Spudich, M. S. Mooseker, and R. E. Cheney, "Myosin-V is a processive actin-based motor," Nature **400,** 590–593 (1999).
7. H. Yin, M. D. Wang, K. Svoboda, R. Landick, S. M. Block, and J. Gelles, "Transcription against an applied force," Science **270,** 1653–1657 (1995).
8. L. Nugent-Glandorf and T. T. Perkins, "Measuring 0.1-nm motion in 1 ms in an optical microscope with differential back-focal-plane detection," Opt. Lett. **29,** 2611–2613 (2004).
9. K. C. Neuman and S. M. Block, "Optical trapping," Rev. Sci. Instrum. **75,** 2787–2809 (2004).
10. E. A. Abbondanzieri, W. J. Greenleaf, J. W. Shaevitz, R. Landick, and S. M. Block, "Direct observation of base-pair stepping by RNA polymerase," Nature **438,** 460–465 (2005).
11. K. M. Herbert, A. La Porta, B. J. Wong, R. A. Mooney, K. C. Neuman, R. Landick, and S. M. Block, "Sequence-resolved detection of pausing by single RNA polymerase molecules," Cell **125,** 1083–1094 (2006).
12. T. T. Perkins, H. W. Li, R. V. Dalal, J. Gelles, and S. M. Block, "Forward and reverse motion of single RecBCD molecules on DNA," Biophys. J. **86,** 1640–1648 (2004).
13. M. D. Wang, M. J. Schnitzer, H. Yin, R. Landick, J. Gelles, and S. M. Block, "Force and velocity measured for single molecules of RNA polymerase," Science **282,** 902–907 (1998).
14. M. D. Wang, H. Yin, R. Landick, J. Gelles, and S. M. Block, "Stretching DNA with optical tweezers," Biophys. J. **72,** 1335–1346 (1997).
15. W. Steffen, D. Smith, R. Simmons, and J. Sleep, "Mapping the actin filament with myosin," Proc. Natl. Acad. Sci. U.S.A. **98,** 14949–14954 (2001).
16. M. Capitanio, R. Cicchi, and F. S. Pavone, "Position control and optical manipulation for nanotechnology applications," Eur. Phys. J. B **46,** 1–8 (2005).
17. K. Visscher, S. P. Gross, and S. M. Block, "Construction of multiple-beam optical traps with nanometer-resolution position sensing," IEEE J. Sel. Top. Quantum Electron. **2,** 1066–1076 (1996).
18. F. Gittes and C. F. Schmidt, "Interference model for back-focal-plane displacement detection in optical tweezers," Opt. Lett. **23,** 7–9 (1998).
19. W. Denk and W. W. Webb, "Optical measurement of picometer displacements of transparent microscopic objects," Appl. Opt. **29,** 2382–2391 (1990).
20. A. Pralle, M. Prummer, E.-L. Florin, E. H. K. Stelzer, and J. K. H. Horber, "Three-dimensional high-resolution particle tracking for optical tweezers by forward scattered light," Microsc. Res. Tech. **44,** 378–386 (1999).
21. We note that our differential BFP detection is immune to common mode fluctuations such as air currents and lens motion. However, a large fraction (40%) of the optical path is not common mode, and the common mode optical elements (excluding the objective) are rigidly attached to the microscope frame or the optical table by custom-made, large-diameter (>38 mm) aluminum posts. Vibrational testing suggests that the current limits in the mechanical stability of our system are the fiber launches and the QPDs, which are independent for each laser; therefore, the second, 850 nm laser represents an independent measurement.
22. The laser diode was driven by custom electronics that stabilized the temperature to ±15 mK/°C ambient temperature variation. The current stability of the driver was 25 ppm/°C. The manufacturer's specification of the laser diode's spectral linewidth is ~0.5 nm FWHM.
23. Unexpectedly, our 850 nm laser performed 100-fold better than its intensity specification even after the PBS and did not require intensity stabilization ($\sigma_I/I = 3 \times 10^{-5}$). Several identical lasers performed only 10% better than specification after the PBS. In general, intensity stabilization will be required to achieve 0.1 nm vertical resolution.
24. K. C. Neuman, E. A. Abbondanzieri, and S. M. Block, "Measurement of the effective focal shift in an optical trap," Opt. Lett. **30,** 1318–1320 (2005).
25. H. Namatsu, Y. Takahashi, K. Yamazaki, T. Yamaguchi, M. Nagase, and K. Kurihara, "Three-dimensional siloxane resist for the formation of nanopatterns with minimum linewidth fluctuations," J. Vac. Sci. Technol. B **16,** 69–76 (1998).
26. K. C. Neuman, E. H. Chadd, G. F. Liou, K. Bergman, and S. M. Block, "Characterization of photodamage to *escherichia coli* in optical traps," Biophys. J. **77,** 2856–2863 (1999).
27. Increasing the laser power created a drift in the positive z direction. Decreasing the laser power caused a negative z drift. This drift corresponded to a movement of the laser focus (set by the objective) relative to the fiducial mark (set by the sample). Furthermore, drift rates increased linearly with the change in laser power. Finally, after ~15 min at a particular laser power the drift would settle, indicating a new equilibrium had been reached. Since all other optical components have >97% transmission at 1064 nm, these data are best explained by the thermal expansion (or contraction) of the objective as the main source of this drift since its transmission at 1064 nm is 59%.
28. K. Svoboda and S. M. Block, "Force and velocity measured for single kinesin molecules," Cell **77,** 773–784 (1994).
29. A. Yildiz, M. Tomishige, R. D. Vale, and P. R. Selvin, "Kinesin walks hand-over-hand," Science **303,** 676–678 (2004).
30. L. Finzi and J. Gelles, "Measurement of lactose repressor-mediated loop formation and breakdown in single DNA molecules," Science **267,** 378–380 (1995).
31. M. E. J. Friese, H. Rubinsztein-Dunlop, N. R. Heckenberg, and E. W. Dearden, "Determination of the force constant of a single-beam gradient trap by measurement of backscattered light," Appl. Opt. **35,** 7112–7116 (1996).